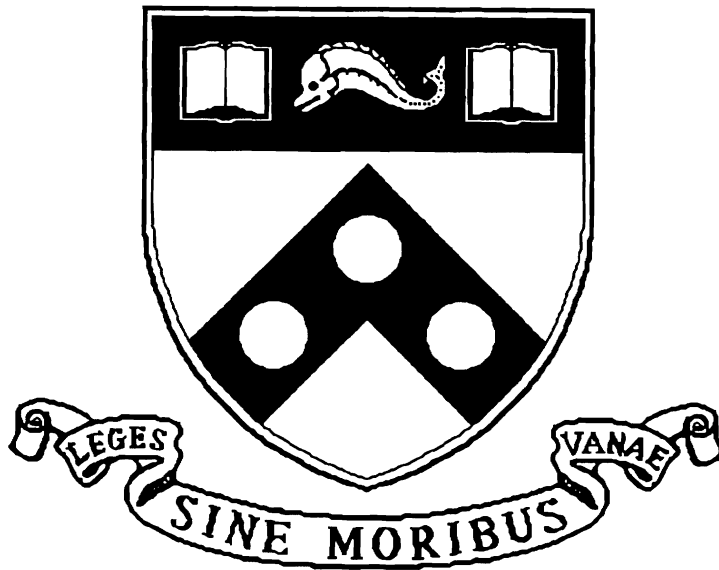


Elastically Deforming a Three-Dimensional Atlas to Match Anatomical Brain Images

MS-CIS-93-53
GRASP LAB 348

Jim C. Gee
Martin Reivich
Ruzena Bajcsy



University of Pennsylvania
School of Engineering and Applied Science
Computer and Information Science Department
Philadelphia, PA 19104-6389

May 1993

Elastically deforming a three-dimensional atlas to match anatomical brain images¹

Jim C. Gee¹, Martin Reivich², and Ruzena Bajcsy¹

Department of Computer and Information Science¹ and
Cerebrovascular Research Center² of the Department of Neurology

University of Pennsylvania
Philadelphia, PA 19104, USA

Abstract

To evaluate our system for elastically deforming a three-dimensional atlas to match anatomical brain images, six deformed versions of an atlas were generated. The deformed atlases were created by elastically mapping an anatomical brain atlas onto different MRI brain image volumes. The mapping matches the edges of the ventricles and the surface of the brain; the resultant deformations are propagated through the atlas volume, deforming the remainder of the structures in the process. The atlas was then elastically matched to its deformed versions. The accuracy of the resultant matches was evaluated by determining the correspondence of 32 cortical and subcortical structures. The system on average matched the centroid of a structure to within 1 mm of its true position and fit a structure to within 11% of its true volume. The overlap between the matched and true structures, defined by the ratio between the volume of their intersection and the volume of their union, averaged 66%. When the gray-white interface was included for matching, the mean overlap improved to 78%; each structure was matched to within 0.6 mm of its true position and fit to within 6% of its true volume. Preliminary studies were also made to determine the effect of the compliance of the atlas on the resultant match.

¹This work was supported by the U.S.P.H.S. under Program Project Grant NS-14867-18.

1 Introduction

The quantitative analysis of cerebral images with the aid of a “computerized” anatomical atlas is under study by different investigators [1-6]. The aim is to improve the accuracy, objectivity, and reproducibility of anatomical localization in anatomical (X-ray computed tomography–CT or magnetic resonance imaging–MRI) and functional (positron emission tomography–PET) images that are difficult to interpret due to inadequate image contrast and limited spatial resolution. In PET, the images additionally lack specific anatomical content.

The assumption underlying atlas-based methods of quantitation is that at a certain level of representation the topological structure of the brain is invariant among normal subjects. The differences between subjects arise only in the details of the shape of the individual brain structures. With these assumptions, the localization problem becomes a problem in matching. Specifically, the objective is to obtain the transformation that will map the atlas to the brain image of the subject, accounting for local shape differences in the process. We have developed a method that uses rigid transformations to correct global misalignment and elastic deformations to resolve local shape differences. Matching is performed in three dimensions without any preference given to the slicing plane.

Broit [7] originated the idea of modeling the atlas as an elastic object and developed the theory for elastically matching a three-dimensional atlas to CT images of the brain. The procedure is intuitive: consider the task of manually deforming a rubber ball to match the shape of some object. In order to alter the shape of the ball, external forces must be applied and sustained. The ball is continually deformed and reshaped until both a satisfactory match is obtained and the applied external forces are equally balanced by the internal forces of the rubber ball resisting the deformation. In our case, the anatomical atlas represents the rubber ball and the brain volume of a subject corresponds to the object. The derivation of the forces for deforming the atlas has previously been described [7,8]. Essentially, the applied forces tend to bring into correspondence the edges of similar cerebral structures in the atlas and the anatomical images.

Kovačić [8] implemented a multiresolution version of Broit’s system, motivated by the observation that larger shape disparities are usually corrected first before finer adjustments are made. The additional advantages of using a coarse-to-fine matching strategy have previously been reported [8]. We evaluate Kovačić’s system in the current study.

The elastic matching system is not interactive during execution but it can be controlled

in three ways. First, the number of deformation cycles is programmed by the user; that is, the user can specify the number of times the elastic matching is invoked to further refine the results produced by the previous deformation cycles. Second, the material compliance of the atlas is controlled by the value of the elastic constant, Lamé's μ [7,8]. For small values of the elastic constant, the atlas is more compliant but the matching is not robust to noise, which may result in unrealistic deformations. Large values of the elastic constant, in contrast, render the atlas more rigid. The applied forces are attenuated and the deformations may be underestimated. This can produce larger residual mismatches. Finally, the choice of brain structures or features to be matched is expressed through the coloring of the atlas [8]. The choice is limited because only a few structures are clearly delineated in the CT or MRI scans. Currently, the edges of the ventricles and the surface of the brain are used for matching and the resultant deformations are propagated through the atlas brain volume, deforming the remainder of the structures in the process.

The present study was designed to determine the accuracy of the matches produced by the elastic matching system. In addition, we made a preliminary evaluation of the effect of the value of the elastic constant on the resultant match.

2 Materials and Methods

In previous work, we compared the outlines of several subcortical structures produced by the elastic matching system with outlines of the same structures manually traced by experts [4,9]. Although the elastic matcher outlines agreed closely with those drawn by the experts, the results were not sufficient to validate the system because we lacked a set of "true" outlines against which both the expert and elastic matcher outlines could be compared. In the current study, we measured the accuracy with which the system matched an atlas to several deformed versions of the atlas. The evaluation was based on comparisons with "true" regional outlines extracted from the deformed atlas volumes.

The anatomical atlas currently used by the elastic matching system was created from a young normal male brain, where outlines for 109 structures were manually traced on 135 myelin-stained sections spaced 700 μm apart. The outlines were then stacked and reformatted to create a three-dimensional anatomical atlas. A representative section overlaid with structural outlines is shown in Figure 1. The atlas described by Dann et al. [4] and used in their evaluation of the elastic matcher is derived from the same anatomical source but is different from the current atlas. The current atlas, however, was constructed using a procedure similar to the one reported in [4].

To evaluate the elastic matching system, six deformed versions of the atlas were generated. The atlas was then matched to its deformed versions. The accuracy of the matches was evaluated by determining the correspondence of several cortical and subcortical regions (see Table 1). The deformed atlases were created by elastically mapping the atlas onto different MRI brain volumes. The six T2-weighted MRI studies used for this purpose were collected from a GE SIGNA 1.5T MRI scanner located at the Hospital of the University of Pennsylvania. The subjects included two men and four women whose neurological status was normal or whose pathology did not involve substantial distortions of normal anatomy. The mean age of the group in years was 67 ($\sigma = 10$). The number of slices for each study ranged from a minimum of 16 to a maximum of 20. Slices were 7.5 mm apart with $0.781 \times 0.781 \text{ mm}^2$ pixels. The MRI brain images were reformatted into three-dimensional image volumes after the skulls in the images were manually removed. The experimental method for the study is illustrated in Figure 2. In the remainder of the paper, the “test” or “experimental” images to which the atlas is matched or elastically mapped will be called “deformed atlases” or “deformed versions of the atlas.”

For the best matching results, the coloring of the atlas should be altered to correspond to the gray value appearance of the brain image to which it is being matched [8]. In practice, however, the ventricles are colored a uniform shade of gray and the rest of the brain is similarly assigned only one gray value. This simple coloring scheme is adequate for matching on the ventricles and the brain surface in anatomical images. The same coloring scheme is used in the current study except in the experiments where we delineated additional structures to examine the effect of using more “information” or features on the resultant elastic match. The original and deformed atlases are colored identically in all the experiments; therefore, any residual mismatches are due to the elastic matching system and not discrepancies in the way the volumes were colored. Figure 3 shows a typical section of one of the deformed atlases and the corresponding slice in the MRI study from which the deformed atlas was created. The atlas section is colored to indicate some of the structures used in the current evaluation.

Matching is implemented as a two-step procedure: the atlas and anatomical image volumes are first aligned globally to remove translational, rotational, and scale differences [8,10]; elastic matching is then performed to correct local shape differences. The outcome of the elastic match therefore depends on the accuracy of the global registration. This confounding effect on the resultant elastic match is removed in the current study since our interest is in the elastic matching component of the system. Note that each deformed atlas volume is created, first, by globally registering the atlas to an MRI brain volume (see “Removal of global registration effects” in Figure 2). This step introduces the global misalignment between the atlas and its deformed version—the remaining deformations applied

to the atlas are localized and do not affect the global alignment (see “Creation of deformed atlas volume” in Figure 2). To correct the global misalignment is trivial—the rigid transformation is the same one used to globally register the atlas to the associated MRI brain image volume. The “globally registered” atlas is then elastically matched to its deformed version. The accuracy of the resultant elastic match was evaluated for the six deformed versions of the atlas.

In every experiment including those described below, three deformation cycles were performed and an intermediate value ($\mu = 0.5$) was used for the elastic constant unless otherwise noted. These are the same values we use in practice and they represent a compromise between the quality of match and the amount of computational time required for each cycle. Note, however, only one deformation cycle was used to produce the deformed versions of the atlas.

In addition to evaluating the accuracy of elastic matching, we examined how its results were affected when the value of the elastic constant or the structures used for matching were altered. The latter effect was studied by matching the atlas a second time to the deformed atlas volume of the fifth case, where, in addition to the ventricles and brain surface, the edges of the cortical and subcortical structures listed in Table 1 were used for matching. This represents the ideal circumstance where the structures to be matched can be identified and segmented in the tomographic images. A more realistic situation, especially for MRI scans, is one where the gray and white matter can easily be distinguished. We repeated the 6 matches above, matching the gray-white interface in addition to the brain surface and cerebrospinal fluid (CSF) spaces.

To study the effect of the material compliance of the atlas on the resultant match, two additional deformed atlases were created using the MRI study from which the fifth case was produced, one using 0.75 for the elastic constant and the second, 0.25 for the elastic constant. For each of the three deformed atlases, three separate matches were performed using large ($\mu = 0.75$), intermediate ($\mu = 0.5$), and small ($\mu = 0.25$) values for the elastic constant respectively.

3 Results

The accuracy of each match was evaluated based on the amount of overlap between the deformed version of the atlas and the elastically mapped atlas. The overlap between two volumes, whether referring to individual structures or whole atlas volumes, is defined as the

ratio between the volume of their intersection and the volume of their union:

$$\text{Overlap}(\text{mapped atlas}, \text{deformed version of atlas}) = \frac{\text{volume of intersection}}{\text{volume of union}} \quad (1)$$

Instead of defining the overlap relative to the true or matched volume, we chose to normalize relative to the union of both volumes. Using the value of the union helps to account for the discrepancy in size between the true and matched volumes. To see why this is important, consider the case where the true volume is entirely within the bounds of a matched volume but is only half its size. For quantitative purposes, the larger size of this matched volume may have a negative effect similar to that of another matched volume which is of equal size to the true volume but only overlaps the true volume by one half. By penalizing both size and overlap discrepancies, our definition of overlap is more conservative. For example, given two volumes of equal size of 1,000 voxels with a half of the voxels (500) overlapping, the overlap defined relative to only one of the volumes is 0.5, but the overlap by our definition is only 0.33.

3.1 Accuracy of Match

Table 1 lists the cortical and subcortical structures used in the evaluation of the 6 matches. Table 2 presents the mean overlap results for the whole atlas volume and the 32 brain structures, averaged over the 6 cases. The mean overlap between the whole atlas volumes after global registration but prior to elastic matching was 85% ($\sigma = 1.4\%$). After elastic matching, all cases were matched with better than 98% overlap between the atlas volumes (mean overlap = 98.3%, $\sigma = 0.2\%$).

The mean overlap, averaged over the 6 cases, for the 32 cortical and subcortical structures after elastic matching was 66% ($\sigma = 16\%$). The final match or overlap improved by more than 100% for 91 (47%) of the 192 structures in the 6 cases. The mean improvement in overlap for the remaining 101 structures was 56%. Among the best matched structures were the cerebellum, pons, medulla, thalamus, midbrain, head of caudate, superior and middle frontal gyri, superior and inferior temporal gyri, and lateral ventricles. The structures that were matched the least successfully included the body of caudate, left putamen, globus pallidus, third ventricle, and angular gyrus (mean overlap = 47%, $\sigma = 12\%$). A typical example of the correspondence of the atlas to one of the deformed atlases before and after elastic matching is shown in Figure 4.

We further evaluated each structural match by measuring the differences in volume and position between the elastically mapped and corresponding true structures. Table 3 summarizes the volumetric percent difference between the matched volume and the true volume of each structure, where the volumetric percent difference is defined as follows:

$$\text{Volumetric percent difference} = \frac{\text{matched volume} - \text{true volume}}{\text{true volume}} \quad (2)$$

For the 6 cases, 100 of the 192 mapped structures showed negative volumetric percent differences with their corresponding true volumes; in other words, 52% of the matched structures were smaller than their true size (mean volumetric percent difference = -8%, $\sigma = 7\%$). The mean volumetric percent difference for the remaining 92 matched structures was 14% ($\sigma = 20\%$). The largest negative volumetric percent difference for any structure was -36% (third ventricle in the first case) and the largest positive percent difference was 155% (left body of caudate in the fourth case). The structures with the largest discrepancy between their matched volume and true volume ($> 10\%$ mean absolute difference) included the body of caudate, left head of caudate, lenticular nucleus, third and fourth ventricles, left precentral gyrus, and left hippocampus. The mean absolute percent difference calculated by averaging the absolute value of each of the percent differences was 11% ($\sigma = 15\%$). On average then each matched volume was approximately 11% larger or smaller than its true size.

The accuracy of the location of a matched structure was measured by calculating the distance from its centroid to the centroid of its corresponding true volume. Table 4 presents the distance measurements for the 6 cases. The largest distance measured for any structure was 3.6 mm (left putamen in the sixth case) and the smallest was 0.1 mm (cerebellum in the first, fourth, and fifth cases and left hippocampus and left angular gyrus in the second case). The structures that were displaced the furthest from their true centroid locations (≥ 1.0 mm difference) included the body of caudate, lenticular nucleus, left thalamus, lateral and third ventricles, left precentral gyrus, left superior temporal gyrus, right hippocampus, and left inferior temporal gyrus (mean distance = 1.4 mm, $\sigma = 0.4$ mm). The mean displacement, averaged over all structures and all cases, was 1.0 mm ($\sigma = 0.7$ mm).

3.2 Match Features

Matching is normally focused on the ventricles and brain surface. We compared the results from one such “normal” match (Match Norm) to the results obtained in the corresponding

ideal situation where every structure under investigation is used as a feature for matching (Match All). For match All the overlap for 22 of the 32 structures improved by over 100% after 3 deformation cycles. The increase in overlap for the remaining 10 structures averaged 68%. When only the brain surface and ventricles were used for matching, 15 structures showed improvements in overlap of over 100%. The mean increase in overlap for the other 17 structures was 54%. The mean structural overlap for match Norm was 61% ($\sigma = 18\%$) and for match All, 74% ($\sigma = 15\%$). Twenty six of the 32 structures were matched more accurately in match All than in match Norm (mean improvement in overlap over match Norm = 43%, $\sigma = 51\%$).

Table 5 presents the mean overlap results for the 6 matches in which the gray-white boundary was used for matching. The mean overlap between the whole atlas volumes after elastic matching was 98.1% ($\sigma = 0.1\%$). The structural overlap averaged 78% ($\sigma = 17\%$). The mean absolute volumetric percent difference was 6% ($\sigma = 10\%$). The structures with the largest discrepancy between their matched volume and true volume ($> 10\%$ mean absolute difference) included the left body and head of caudate and the third and fourth ventricles. The right body of caudate and third and fourth ventricles were also the mapped structures that were displaced the furthest from their true centroid locations (mean distance = 2.6 mm, $\sigma = 2.4$ mm). In the third match, the mapped volume for the third ventricle was misplaced 10.7 mm. The mean distance, averaged over the 6 cases, between the centroid of a mapped structure and its true location was 0.6 mm ($\sigma = 1.0$ mm).

3.3 Elastic Constant

Three deformed atlas volumes were created from the fifth MRI study, each using an atlas with a different material stiffness: compliant (small-valued elastic constant, $\mu = 0.25$), elastic (intermediate-valued elastic constant, $\mu = 0.5$), and rigid (large-valued elastic constant, $\mu = 0.75$). The same three atlases of varying stiffness were matched to each deformed atlas volume. A one-way analysis of variance (ANOVA) was conducted to analyze the differences in mean structural overlap between the matched atlases for each deformed atlas. Differences in the volume and location of a mapped structure were similarly analyzed with one-way ANOVA's. The F values for both the mean structural location and overlap are presented in Table 6. The results of the 9 one-way ANOVA's indicated that none of the differences were significant ($p > 0.25$).

To study the agreement among the matched atlases for each deformed atlas, the amount of overlap between each pair of matched atlases was determined and the mean results are presented in Table 7. The distance between the centroids of the corresponding structure

in each pair of matched atlases was also calculated and the mean results are included in Table 7.

To determine the agreement in size among the corresponding structures in the three matches for each deformed atlas, the percent standard deviation, defined by the ratio between the standard deviation and its corresponding mean value, was calculated for each structure. The mean value refers to the average volumetric size of the corresponding structure in the three matched atlases. For the three matches to the deformed atlas generated from a compliant atlas, the mean volumetric percent standard deviation was 4%; on average then the three matched volumes for each structure were approximately 4% larger or smaller than one another. The mean volumetric percent standard deviation for the matches to the deformed atlas generated from an elastic atlas was 4% and for the matches to the deformed atlas generated from a rigid atlas, 2%.

Finally, we pairwise compared the deformed atlases, which represent the elastically matched atlases to a typical MRI study (fifth case in the current study). Table 8 presents the mean structural overlap for each pairwise comparison and also includes information about the mean distance between the centroids of corresponding structures. The mean volumetric percent standard deviation for the 3 deformed atlases was 9%.

4 Discussion

The system was generally more successful in matching the larger structures than in matching the smaller ones. The overlap measure, however, is biased against smaller structures: mismatches in them have a larger relative effect on the ratio between the amount of overlap and non-overlap than mismatches in larger structures. More accurate matches were also obtained for structures that are more compact and regular in shape. This is evident in the results for the ventricles, where an accurate correspondence was expected since the system attempts specifically to match these structures. The relatively large-sized lateral ventricles were well matched with a mean overlap of 72% but the overlap averaged only 48% for the much smaller third and fourth ventricles (see Table 2). As expected, when the structure itself was used for matching, its correspondence was generally much better than the correspondence from matching only on the brain surface and ventricles—the mean structural overlap was 22% larger in the match where the structure itself was used for matching.

The data used in the early development of the elastic matching technique consisted exclusively of X-ray CT images. The ventricles were obvious structures for matching because

of their medial location within the brain and their relatively well defined appearance in the CT images. The current study shows that matching strictly on the brain surface and ventricles produces satisfactory region of interest outlines for the larger brain regions but may be inadequate for accurately outlining smaller structures or ones with very irregular shapes. The last result in the paragraph above points out the obvious: the more information or features provided to the matching algorithm, the more accurate and reliable is the resultant match. In the case of MRI, techniques exist that can automatically distinguish between gray and white matter in addition to identifying the CSF spaces [11-13]. As Tables 2 and 5 illustrate, the inclusion of the gray-white boundary in matching substantially improves the correspondence between the matched and true structures. When the gray-white boundary was included, the system on average matched the centroid of a structure to within 0.6 mm of its true position and fit a structure to within 6% of its true volume. Matching only on the ventricles and brain surface, the mean distance between the centroids increased to 1 mm and the mean volumetric percent difference approximately doubled to 11%.

It was noted earlier that matches using a more rigid atlas are more robust to noise and less likely to include unrealistic deformations. The trade-off is that the residual mismatch may increase with the stiffness of the atlas. Three atlases of varying compliance were matched to the same MRI source to create 3 deformed atlases. Each deformed atlas was matched 3 times using the same 3 atlases from which the deformed atlases were generated. In all 9 matches were performed. The ANOVA results show that within each case no significant differences were found between the three matched atlases. This indicates that no particular penalty is incurred for choosing larger values for the elastic constant. We pairwise compared the 3 matches for each of the deformed atlases to study the agreement among the results (see Table 7). In general, the agreement between the matches using the elastic atlas ($\mu = 0.5$) and the rigid atlas ($\mu = 0.75$) was largest; the worst agreement, as expected, was between the matches using the compliant atlas ($\mu = 0.25$) and the rigid atlas.

We also measured the variability in the results for a “real” case, where the 3 atlases of different stiffness were matched to an MRI brain volume (see Table 8). The matched atlases in this case follow the same pattern of agreement observed in the results for the 3 deformed atlases. There is, however, a larger discrepancy in agreement between the matches. This may be a consequence of using only one deformation cycle instead of the usual three to match the atlases to the MRI brain volume.

Although the compliance of the atlas can be adjusted to have an extreme effect on the resultant elastic match, it should be made clear that the “parameters” bearing the most influence on the successful outcome of a match are the features made available to the algorithm. The main point about the elastic constant is that selecting a larger value

and, hence, a more rigid atlas ensures a solution that is less sensitive to noise without an appreciable compromise in accuracy.

A tenet of our approach to anatomical localization is that relying only on global registration algorithms may be inadequate when using atlases that do not encode information about normal anatomical variation. In the current study, the mean structural overlap, averaged over all structures and all cases, obtained by global registration was 32% ($\sigma = 18\%$). The structural correspondence improves two-fold when the volumes are additionally submitted to elastic matching (mean structural overlap = 66%)—recall that prior to elastic matching, the atlas is globally aligned with each deformed atlas volume. The improvement in correspondence is even larger if the gray-white boundary is available for matching (mean structural overlap = 78%).

It is of interest to note the accuracy with which the atlas is matched to the 6 deformed versions of the atlas when both global and elastic matching are performed. In this case, we omitted the step to correct the global misalignment prior to matching (see stage 1 of Figure 2). The mean structural overlap after both global and elastic matching was 62% ($\sigma = 17\%$). On average the centroid of a structure was matched to within 1.0 mm ($\sigma = 1.0$ mm) of its true position and a structure was fit to within 11% ($\sigma = 14\%$) of its true volume. Despite these results, the objective of the current study was not to establish that our 2-step elastic matching procedure is superior to global registration techniques for anatomical localization. A comparative study of different methods is a much more complicated endeavor and would have to address issues such as the validity of the atlas and the preprocessing requirements of each approach. Another important issue is the method of evaluation and some comment is necessary on the one we have designed for the present study. As described earlier, our previous evaluations defined the accuracy of elastic matching relative to the performance of a group of experts. To conduct a more objective evaluation, deformed versions of the atlas were used in the present study. However, the morphometric variation introduced into each deformed atlas is produced by the same elastic matching algorithm that is under investigation. The current evaluation then in part measures the consistency with which the volumes are deformed.

Our approach is not without its disadvantages. The elastic matching process is computationally intensive, but we have begun to investigate other numerical methods to complement our multiresolution approach. The preprocessing to prepare the images for elastic matching is time consuming and is currently not entirely automated. A more important deficiency in the practical use of the system is the coloring of the atlas, which in order to obtain the best matching results should correspond to the gray value appearance of the CT or MRI brain images. We are studying an approach that abandons the use of gray value inten-

sity correlation in favor of features that can be acquired from various tissue classification algorithms.

In summary, the elastic matching technique demonstrated on average a two-fold improvement in correspondence of a variety of cortical and subcortical regions in matches to 6 deformed atlas volumes. Variables important in quantitative analysis such as region size and location were examined. The system on average matched the centroid of a structure to within 1 mm of its true position and fit a structure to within 11% of its true volume. When the gray-white interface was matched in addition to the ventricles and brain surface, the mean overlap improved to 78%; each structure was matched to within 0.6 mm of its true position and fit to within 6% of its true volume. Our method of anatomical localization based on elastic matching satisfies a majority of the criteria proposed by Mazziotta and Koslow for PET image analysis [14]. Rottenberg [15] proposed that for each data analysis approach its objective, logic, and details of implementation should be explicitly addressed and we have done so in previous reports [4,7,8,10]. Finally, our approach is specifically designed to account for morphometric variations in neuroanatomy that cannot be described by a proportional linear scale, a capability recommended by the PET Data Analysis Working Group [16]. In the case of substantial anatomical variation, the elastic matching would need human guidance for the best results.

References

- [1] Evans AC, Beil C, Marrett S, Thompson CJ, Hakim A. Anatomical-Functional Correlation Using an Adjustable MRI-Based Region of Interest Atlas with Positron Emission Tomography. *J Cereb Blood Flow Metab* 1988;8(4):513–30.
- [2] Evans AC, Dai W, Collins L, Neelin P, Marrett S. Warping of a computerized 3-D atlas to match brain image volumes for quantitative neuroanatomical and functional analysis. In: Loew MH, ed, *Medical Imaging V: Image Processing*. Washington: SPIE, 1991:236–46.
- [3] Bohm C, Greitz T, Seitz R, Eriksson L. Specification and Selection of Regions of Interest (ROIs) in a Computerized Brain Atlas. *J Cereb Blood Flow Metab* 1991;11:A64–8.
- [4] Dann R, Hoford J, Kovačič S, Reivich M, Bajcsy R. Evaluation of Elastic Matching System for Anatomic (CT, MR) and Functional (PET) Cerebral Images. *J Comput Assist Tomogr* 1989;13(4):603–11.

- [5] Herholz K, Pawlik G, Wienhard K, Heiss W-D. Computer Assisted Mapping in Quantitative Analysis of Cerebral Positron Emission Tomograms. *J Comput Assist Tomo* 1985;9(1):154–61.
- [6] Fox PT, Perlmutter JS, Raichle ME. A Stereotactic Method of Anatomical Localization for Positron Emission Tomography. *J Comput Assist Tomo* 1985;9(1):141–53.
- [7] Broit C. Optimal Registration of Deformed Images. *Doctoral dissertation, University of Pennsylvania, PA* 1981.
- [8] Bajcsy R, Kovačič S. Multiresolution Elastic Matching. *Comput Vision, Graphics, Image Process* 1989;46(1):1–21.
- [9] Gee JC, Reivich M, Bilaniuk L, Hackney D, Zimmerman R, Kovačič S, Bajcsy R. Evaluation of multiresolution elastic matching using MRI data. In: Loew MH, ed, *Medical Imaging V: Image Processing*. Washington: SPIE, 1991:226–34.
- [10] Kovačič S, Gee JC, Ching WSL, Reivich M, Bajcsy R. Three-dimensional registration of PET and CT images. In: Kim Y, Spelman FA, eds, *Proceedings of the Annual International Conference of the IEEE EMBS*. New York: IEEE, 1989:548–9.
- [11] Choi HS, Haynor DR, Kim Y. Partial Volume Tissue Classification of Multi-channel Magnetic Resonance Images—A Mixel Model. *IEEE Trans Med Imaging* 1991;10(3):395–407.
- [12] Lachmann F, Barillot C. Brain Tissue Classification from MRI Data by Means of Texture Analysis. To appear in: Loew MH, ed, *Medical Imaging VI: Image Processing*. Washington: SPIE, 1992.
- [13] Chen SY, Lin WC, Chen CT. Split-and-Merge Image Segmentation Based on Localized Feature Analysis and Statistical Tests. *CVGIP: Graphical Models and Image Processing* 1991;53(5):457–75.
- [14] Mazziotta JC, Koslow SH. Assessment of goals and obstacles in data acquisition and analysis from emission tomography: report of a series of international workshops. *J Cereb Blood Flow Metab* 1987;7:1–31.
- [15] Rottenberg DA. Proceedings of the PET Data Analysis Workshop, general introduction. *J Cereb Blood Flow Metab* 1991;11:A1–A2.
- [16] Rapoport SI. Discussion of PET Workshop reports, including recommendations of PET Data Analysis Working Group. *J Cereb Blood Flow Metab* 1991;11:A140–6.



Figure 1. A section of the digitized brain used to create the anatomical atlas, overlaid with structural outlines. Outlines for 109 structures were manually traced on 135 myelin-stained sections ($700\ \mu\text{m}$ thickness) from a young normal male brain. The outlines were then stacked and reformatted to create a three-dimensional anatomical atlas.

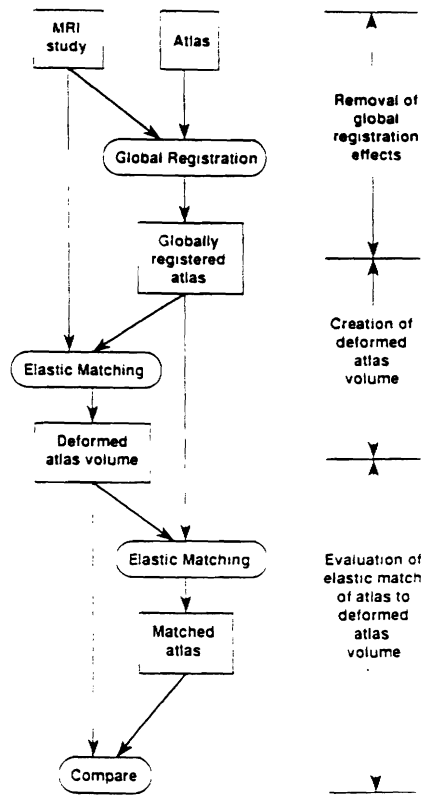


Figure 2. Experimental method for evaluating the accuracy of the elastic matching system. The procedure can be divided into 3 stages as illustrated in the figure. First, the effects due to global mismatch are removed by ensuring that the atlas to be used for elastic matching is in global register with the MRI brain image used to create the deformed atlas. Prior to registration and after the skull in the images have been manually removed, the MRI images are reformatted into a three-dimensional image volume. The deformed atlas is created in the second stage by elastically deforming the globally registered atlas to match the MRI brain volume. To obtain the best matching results, the coloring of the atlas should be altered to correspond to the gray value appearance of the brain image to which it is being matched. In practice, however, the ventricles are colored a uniform shade of gray and the rest of the brain is similarly assigned only one gray value. This simple coloring scheme is adequate for matching on the ventricles and brain surface. In the final stage, the original atlas, now in global register with its deformed version, is elastically matched to the deformed atlas. Both atlas volumes are identically colored; therefore, any residual mismatches are due to the elastic matching system and not discrepancies in the way the volumes were colored. The accuracy of the match between the two volumes is evaluated by comparing the overlap of their outlines for the brain surface and 32 cortical and subcortical structures.

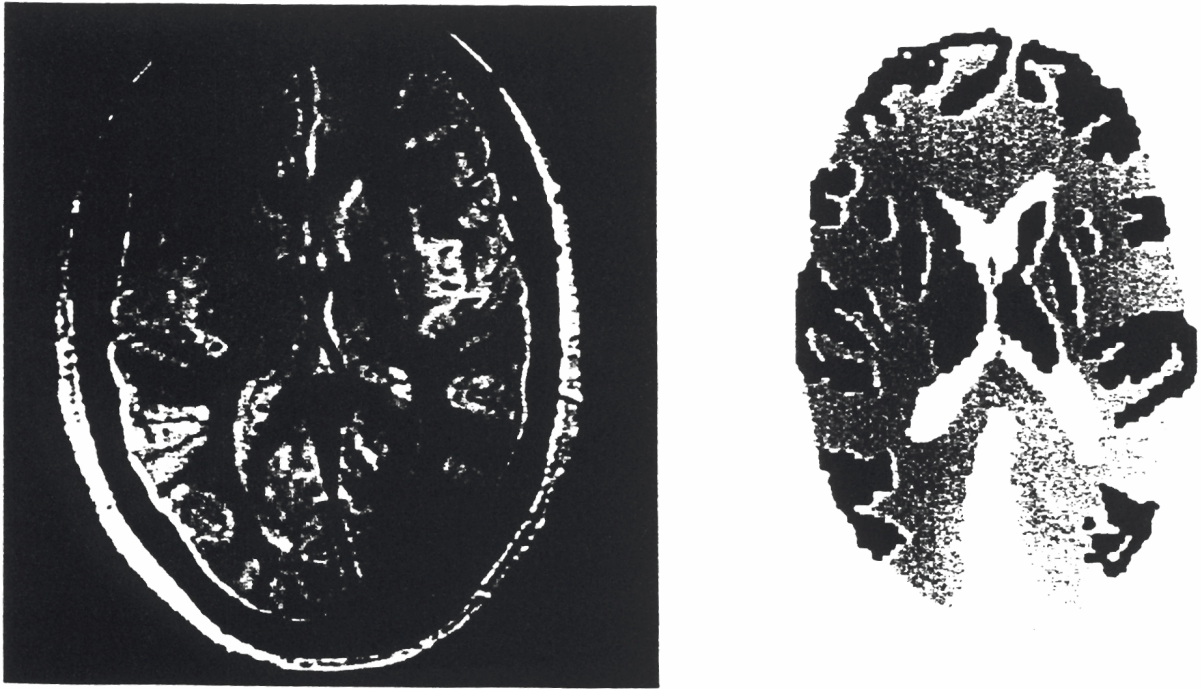


Figure 3. (Right) A typical section of one of the deformed atlases and (Left) the corresponding slice in the MRI study from which the deformed atlas was created. The atlas section is colored to indicate some of the structures used in the current evaluation.



Figure 4a. Example of the correspondence of the atlas to one of its deformed versions before and after elastic matching. Shown are two identical slices of the deformed atlas from case 2. The outlines on the left represent the structural contours of the atlas after only global registration to the deformed atlas has been performed. The outlines on the right are the contours of the atlas after elastic matching to the deformed atlas.



Figure 4b. Same as (a) except slices are from a different level of the deformed atlas.

Table 1: Brain structures used in the evaluation of the elastic matching system.

Structure Code	Structure Name
111	Left body of caudate
112	Right body of caudate
131	Left head of caudate
132	Right head of caudate
135	Left putamen
136	Right putamen
137	Left globus pallidus
138	Right globus pallidus
117	Left thalamus
118	Right thalamus
201	Cerebellum
301	Midbrain
311	Pons
321	Medulla
503	Left lateral ventricle
504	Right lateral ventricle
505	Third ventricle
507	Fourth ventricle
17	Left precentral gyrus
18	Right precentral gyrus
5	Left superior frontal gyrus
6	Right superior frontal gyrus
35	Left superior temporal gyrus
36	Right superior temporal gyrus
147	Left hippocampus
148	Right hippocampus
7	Left middle frontal gyrus
8	Right middle frontal gyrus
39	Left inferior temporal gyrus
40	Right inferior temporal gyrus
51	Left angular gyrus
52	Right angular gyrus

For brevity, a code is associated with each structure and is used in place of the full name of the structure in subsequent tables.

Table 2: Mean overlap between the matched and true volumes of each structure.

Structure	Before matching		1st Deform.		2nd Deform.		3rd Deform.	
	Mean	σ	Mean	σ	Mean	σ	Mean	σ
brain	0.85	0.01	0.97	0.00	0.98	0.00	0.98	0.00
111	0.01	0.03	0.19	0.13	0.29	0.09	0.39	0.09
112	0.13	0.04	0.35	0.06	0.50	0.03	0.53	0.04
131	0.34	0.15	0.61	0.10	0.68	0.06	0.73	0.05
132	0.18	0.19	0.48	0.11	0.64	0.07	0.66	0.06
135	0.37	0.05	0.51	0.14	0.54	0.13	0.54	0.14
136	0.33	0.05	0.54	0.10	0.60	0.11	0.60	0.11
137	0.21	0.05	0.38	0.14	0.42	0.14	0.41	0.14
138	0.14	0.05	0.39	0.11	0.45	0.11	0.45	0.10
117	0.46	0.08	0.70	0.08	0.74	0.06	0.76	0.07
118	0.50	0.08	0.73	0.05	0.79	0.04	0.79	0.03
201	0.64	0.06	0.91	0.00	0.95	0.01	0.95	0.01
301	0.41	0.16	0.68	0.08	0.74	0.07	0.74	0.06
311	0.34	0.16	0.77	0.05	0.83	0.05	0.85	0.05
321	0.42	0.12	0.82	0.02	0.88	0.03	0.88	0.02
503	0.21	0.09	0.55	0.04	0.69	0.02	0.74	0.02
504	0.17	0.09	0.47	0.07	0.68	0.03	0.71	0.04
505	0.05	0.08	0.28	0.10	0.38	0.15	0.39	0.13
507	0.01	0.02	0.34	0.13	0.53	0.07	0.56	0.09
17	0.50	0.09	0.69	0.07	0.71	0.08	0.70	0.08
18	0.38	0.07	0.60	0.09	0.63	0.10	0.63	0.10
5	0.34	0.09	0.65	0.05	0.71	0.05	0.71	0.05
6	0.44	0.05	0.67	0.04	0.71	0.04	0.72	0.04
35	0.48	0.14	0.71	0.09	0.73	0.08	0.73	0.08
36	0.47	0.07	0.74	0.08	0.78	0.07	0.78	0.08
147	0.23	0.24	0.55	0.20	0.58	0.15	0.61	0.16
148	0.28	0.21	0.50	0.18	0.59	0.18	0.62	0.19
7	0.46	0.10	0.72	0.04	0.75	0.04	0.75	0.04
8	0.40	0.07	0.68	0.07	0.73	0.08	0.73	0.07
39	0.30	0.10	0.59	0.05	0.64	0.03	0.65	0.04
40	0.35	0.10	0.66	0.09	0.72	0.06	0.73	0.05
51	0.44	0.11	0.53	0.10	0.54	0.11	0.54	0.12
52	0.27	0.10	0.48	0.13	0.52	0.11	0.51	0.10

For each case, the overlaps for the whole atlas volume and the structures listed in Table 1 were calculated prior to matching and after each of the 3 deformation cycles during the match. The results were then averaged over the 6 cases to produce the values reported here. The values for the row marked “brain” represent the overlap results for the whole atlas volume.

Table 3: Volumetric percent difference between the matched and true volumes of each structure.

Structure	Case 1	Case 2	Case 3	Case 4	Case 5	Case 6	Absolute Mean
111	0.0	-6.1	-0.8	155.4	16.3	39.8	36.4
112	-17.5	-2.8	6.1	3.4	46.8	26.6	17.2
131	-6.7	4.3	3.0	11.0	31.7	20.1	12.8
132	-8.7	-4.6	-2.9	-9.5	-1.3	27.3	9.0
135	13.3	17.8	18.9	20.4	48.2	23.3	23.6
136	17.4	2.1	24.0	2.4	33.6	12.1	15.3
137	22.2	26.5	44.4	26.3	55.8	37.0	35.4
138	7.0	0.7	35.9	18.4	35.7	20.3	19.7
117	-2.4	1.2	0.3	4.8	13.9	14.7	6.2
118	-3.5	-1.9	11.4	1.1	10.5	12.8	6.9
201	0.2	1.1	0.2	0.8	0.9	2.2	0.9
301	-0.1	0.5	-6.9	1.5	0.4	0.9	1.7
311	0.0	-1.2	-7.7	-3.0	-5.7	1.7	3.2
321	-2.0	-2.7	-2.0	-3.5	0.8	-9.5	3.4
503	-14.3	-10.5	2.1	6.4	7.1	14.2	9.1
504	-11.5	-13.1	2.3	-1.9	-0.6	13.7	7.2
505	-36.3	-29.9	-17.9	-18.7	-35.2	23.2	26.9
507	31.6	12.6	52.9	14.6	-8.2	-7.1	21.2
17	-1.1	-8.2	-14.8	-14.0	-21.4	-7.0	11.1
18	2.3	3.7	-14.3	3.2	-2.2	-1.3	4.5
5	2.2	-2.9	-14.8	-10.5	-8.1	-12.1	8.4
6	1.2	-3.5	-17.1	-7.4	-6.6	-14.6	8.4
35	-1.4	-4.1	-4.7	-3.8	-12.9	-5.5	5.4
36	-0.9	0.4	-10.9	0.2	-5.4	-4.2	3.7
147	-11.6	-7.4	9.4	12.2	-17.1	-11.9	11.6
148	-9.1	-9.3	5.0	-3.2	-13.5	-2.2	7.1
7	1.8	-7.1	-11.8	-14.9	-10.7	-4.8	8.5
8	3.6	0.2	-11.7	-3.6	-2.4	-5.1	4.4
39	1.2	-5.8	13.8	-14.1	0.3	-0.4	5.9
40	-4.5	-3.5	5.1	-6.9	-4.7	0.8	4.3
51	-4.0	-3.0	0.2	-0.5	-6.9	2.1	2.8
52	-6.9	-7.8	-6.6	-6.9	-4.5	4.2	6.1

The accuracy of each structural match was additionally evaluated by calculating the volumetric percent difference between the final matched volume and the true volume (see Equation 2). A negative percent difference indicates that the volume matched by the system is smaller than its true size. A positive difference indicates the matched volume is larger than the true volume. The last column shows the mean absolute percent difference for each structure, averaged over the 6 cases.

Table 4: Distance between the matched and true centroids of each structure.

Structure	Case 1	Case 2	Case 3	Case 4	Case 5	Case 6	Mean
111	1.7	0.9	1.7	0.8	0.7	1.9	1.3
112	2.1	0.6	1.7	1.4	0.6	1.0	1.2
131	0.4	0.6	0.7	0.9	1.6	1.1	0.9
132	0.6	0.6	0.5	0.6	0.3	1.5	0.7
135	0.6	1.2	2.5	2.2	2.6	3.6	2.1
136	1.2	1.5	2.8	1.4	0.9	3.0	1.8
137	1.0	1.1	2.3	2.1	2.3	3.1	2.0
138	1.6	1.3	2.4	1.7	1.8	3.1	2.0
117	0.9	0.5	1.5	0.9	1.3	1.4	1.1
118	0.7	0.6	1.3	0.6	0.9	1.4	0.9
201	0.1	0.2	0.2	0.1	0.1	0.2	0.2
301	0.4	0.8	0.9	1.1	0.6	0.8	0.8
311	0.2	0.4	0.4	0.5	0.6	0.6	0.4
321	0.4	0.4	0.3	0.3	0.3	0.6	0.4
503	1.4	0.9	1.1	0.5	1.7	0.5	1.0
504	0.6	1.3	0.9	1.6	0.9	2.5	1.3
505	1.4	1.1	2.0	1.5	1.6	1.0	1.4
507	1.3	1.1	0.4	0.3	0.9	1.1	0.9
17	0.5	0.6	1.6	0.9	1.2	1.1	1.0
18	0.7	0.6	1.2	0.8	1.7	0.4	0.9
5	0.5	0.5	0.6	0.9	1.7	0.4	0.8
6	0.7	0.8	1.3	0.6	1.1	0.6	0.9
35	0.5	1.0	2.5	1.1	1.6	0.8	1.2
36	0.2	0.2	1.9	0.8	0.2	0.6	0.6
147	0.4	0.1	1.7	0.6	1.2	1.1	0.9
148	1.1	0.9	1.0	1.3	2.3	0.4	1.2
7	0.3	0.4	0.7	1.7	1.2	0.8	0.9
8	0.3	0.5	2.0	1.3	0.8	0.7	0.9
39	0.7	0.8	1.2	3.2	0.8	1.5	1.4
40	0.8	0.6	1.1	0.8	0.9	0.6	0.8
51	0.6	0.1	1.7	0.3	1.0	1.0	0.8
52	1.3	0.8	0.8	0.7	1.2	0.8	0.9

To evaluate the accuracy of the location of the matched structures in the 6 cases, the centroid for each matched structural volume was calculated and the Euclidean distance to the centroid of its corresponding true volume was measured. The last column shows the mean distance between the matched and true centroids for each structure, averaged over the 6 cases. All values are in units of millimeters.

Table 5: The effect of including the gray-white interface on the resultant elastic match.

Structure	Before matching		1st Deform.		2nd Deform.		3rd Deform.	
	Mean	σ	Mean	σ	Mean	σ	Mean	σ
111	0.01	0.03	0.48	0.18	0.59	0.10	0.64	0.12
112	0.07	0.07	0.56	0.07	0.63	0.07	0.64	0.05
131	0.29	0.12	0.71	0.08	0.75	0.06	0.77	0.06
132	0.16	0.17	0.64	0.08	0.74	0.05	0.76	0.06
135	0.36	0.15	0.77	0.05	0.83	0.02	0.84	0.03
136	0.25	0.11	0.79	0.05	0.84	0.02	0.84	0.03
137	0.17	0.11	0.68	0.03	0.77	0.03	0.78	0.04
138	0.11	0.05	0.69	0.05	0.76	0.05	0.76	0.04
117	0.47	0.09	0.80	0.03	0.86	0.03	0.86	0.02
118	0.51	0.12	0.85	0.02	0.87	0.02	0.87	0.02
201	0.66	0.10	0.92	0.01	0.95	0.00	0.95	0.00
301	0.37	0.18	0.77	0.03	0.85	0.01	0.87	0.02
311	0.32	0.23	0.73	0.06	0.80	0.03	0.81	0.03
321	0.41	0.21	0.81	0.02	0.87	0.03	0.88	0.03
503	0.19	0.05	0.68	0.04	0.73	0.04	0.73	0.04
504	0.13	0.08	0.61	0.05	0.69	0.02	0.71	0.03
505	0.00	0.00	0.23	0.17	0.33	0.12	0.36	0.17
507	0.07	0.08	0.24	0.10	0.32	0.15	0.34	0.14
17	0.34	0.06	0.79	0.02	0.82	0.02	0.83	0.01
18	0.23	0.05	0.72	0.05	0.77	0.03	0.78	0.03
5	0.25	0.04	0.74	0.02	0.82	0.02	0.82	0.02
6	0.30	0.04	0.78	0.02	0.84	0.02	0.84	0.02
35	0.35	0.09	0.83	0.03	0.87	0.02	0.86	0.02
36	0.29	0.07	0.82	0.03	0.85	0.02	0.85	0.02
147	0.15	0.07	0.67	0.10	0.76	0.05	0.78	0.04
148	0.10	0.07	0.71	0.08	0.78	0.04	0.79	0.04
7	0.39	0.05	0.81	0.01	0.86	0.01	0.86	0.01
8	0.29	0.06	0.79	0.02	0.84	0.02	0.85	0.01
39	0.23	0.08	0.74	0.04	0.81	0.02	0.81	0.02
40	0.16	0.06	0.74	0.04	0.81	0.02	0.81	0.02
51	0.30	0.10	0.78	0.04	0.81	0.03	0.81	0.02
52	0.15	0.06	0.65	0.05	0.75	0.02	0.75	0.03

For each case, the amount of overlap for the structures listed in Table 1 were calculated prior to matching and after each of the 3 deformation cycles during the match. The results were then averaged over the 6 cases to produce the values reported here. Note that the overlap values before matching differ from those in Table 2. This discrepancy is a result of the different coloring scheme that was used to include the gray-white interface for matching. The overlap values shown here before matching are smaller than those in Table 2; therefore, the improvement in correspondence as a consequence of matching the gray-white interface is larger than what it appears to be when only the last two columns of Tables 2 and 5 are compared.

Table 6: One-way ANOVA analyses of the matches in which different values of the elastic constant were used.

		Compliant atlas	Elastic atlas	Rigid atlas
Compliant deformed atlas	N	32	32	32
	Structural overlap			
	M	0.54	0.52	0.51
	σ	0.21	0.21	0.20
	$F =$	0.110		
	Distance between centroids			
	M	1.47	1.65	1.83
	σ	0.95	1.09	1.16
	$F =$	0.914		
	Elastic deformed atlas	N	32	32
Structural overlap				
M		0.61	0.61	0.61
σ		0.18	0.18	0.17
$F =$		0.004		
Distance between centroids				
M		1.08	1.14	1.21
σ		0.58	0.62	0.68
$F =$		0.368		
Rigid deformed atlas		N	32	32
	Structural overlap			
	M	0.65	0.66	0.66
	σ	0.15	0.15	0.14
	$F =$	0.032		
	Distance between centroids			
	M	1.03	0.97	1.02
	σ	0.70	0.54	0.68
	$F =$	0.098		

Three atlases of different compliance were matched to the same MRI source to create the Compliant, Elastic, and Rigid deformed atlases. Each deformed atlas was matched 3 times using the same 3 atlases (Compliant, Elastic, and Rigid) from which the deformed atlases were generated. A one-way analysis of variance (ANOVA) was conducted to analyze the differences in mean structural overlap between the matched atlases for each deformed atlas. Differences in the location of a mapped structure, defined by the distance between its centroid and the centroid of its corresponding true volume, were similarly analyzed with one-way ANOVA's. A significance level of 0.25 was used to minimize the Type II error. Values for the distance statistics are in units of millimeters.

Table 7: Pairwise comparisons of the matches in which different values of the elastic constant were used.

	Pair		Compliant deformed atlas		Elastic deformed atlas		Rigid deformed atlas	
			Mean	σ	Mean	σ	Mean	σ
Overlap agreement	Compliant	Elastic	0.79	0.11	0.81	0.11	0.82	0.08
	Elastic	Rigid	0.83	0.09	0.85	0.08	0.86	0.07
	Rigid	Compliant	0.74	0.13	0.76	0.14	0.79	0.09
Distance between centroids	Compliant	Elastic	0.61	0.85	0.51	0.44	0.47	0.40
	Elastic	Rigid	0.46	0.40	0.33	0.21	0.41	0.41
	Rigid	Compliant	0.98	1.06	0.75	0.49	0.60	0.39

Three atlases of different compliance were matched to the same MRI source to create the Compliant, Elastic, and Rigid deformed atlases. Each deformed atlas was matched 3 times using the same 3 atlases (Compliant, Elastic, and Rigid) from which the deformed atlases were generated. For each deformed atlas, the agreement among the matched atlases was determined by calculating the amount of structural overlap between each pair. In addition, the distance between the centroids of the corresponding structure in each pair of matched atlases was calculated. Shown here are the mean values averaged over the 32 structures. Values for the distance statistics are in units of millimeters.

Table 8: Pairwise comparisons of the matches to an MRI brain image in which different values of the elastic constant were used.

Pair		Structural overlap		Distance between centroids	
		Mean	σ	Mean	σ
Compliant	Elastic	0.62	0.17	1.17	0.76
Elastic	Rigid	0.73	0.12	0.80	0.52
Rigid	Compliant	0.52	0.19	1.74	1.18

Three atlases of different compliance (Compliant, Elastic, and Rigid) were matched to the same MRI brain volume to study the effect of the value of the elastic constant on the resultant match. The agreement among the matched atlases was determined by calculating the amount of overlap between each pair. In addition, the distance between the centroids of the corresponding structure in each pair of matched atlases was calculated. Shown here are the mean values averaged over the 32 structures. Values for the distance statistics are in units of millimeters.